Journal of Research in Science and Engineering (JRSE)
ISSN: 1656-1996 Volume-7, Issue-6, June 2025
DOI: 10.53469/jrse.2025.07(06).12

Development of a Gamma Oscillation-Synchronized 40Hz Audiovisual Stimulation Device

Bo Deng

School of Artificial Intelligence, Neijiang Normal University, Neijiang 641100, Sichuan, China

Abstract: ***Based on the neuromodulatory mechanism of gamma oscillations, this study designed a 40 Hz audiovisual intervention device to improve cognitive function in patients with chronic disorders of consciousness. The device delivers synchronized audiovisual stimulation: auditory stimuli are triggered 2 ms after visual stimulus onset, generating 40 Hz steady-state pulses with sound intensity of 60-80 dB and blue light at 472 nm wavelength (0.03 mW/cm²). The hardware incorporates an STM32L1 microcontroller, DAC8830 digital-to-analog converter, MIX3022 audio amplifier, and voltage-controlled constant-current LED driver circuit. Software-controlled PWM dimming and timer interrupts achieve audiovisual synchronization. Integrated within a wearable eye mask, the device features a bone-conduction speaker and lens-focused LED. Testing confirmed precise audiovisual synchronization (2 ms delay) and stable audio waveforms, demonstrating compliance with safety standards and providing a novel non-invasive approach for neurological disorder treatment.***

Keywords: Gamma Oscillations, 40Hz, Synchronized Audiovisual Stimulation, Wearable Eye Mask.

1. Introduction

Gamma oscillations, characterized by high-frequency neural activity ranging from 30 to 100 Hz, are closely associated with complex brain functions including consciousness generation, cognitive processing, and information integration [1][2]. Adrian first recorded gamma oscillations in the olfactory bulb of anesthetized hedgehogs in 1942, observing that intense olfactory stimulation induced a shift to low-amplitude, approximately 50 Hz discharge activity [3][4]. During cognitive tasks, gamma oscillations exhibit high-intensity activity correlated with psychological states such as focus, alertness, and memory. Multiple brain regions—including the cerebral cortex, hippocampus, and gallbladder—differentially contribute to the generation and modulation of these oscillations. The relationship between gamma oscillations and higher-order brain functions is increasingly understood, with aberrant gamma activity observed across various neuropsychiatric disorders. Abnormal gamma oscillations are strongly linked to central nervous system pathologies, including Alzheimer's disease, Parkinson's disease, and schizophrenia. Studies indicate that sensory stimulation-induced 40 Hz gamma oscillations may confer neuroprotective effects [5][6]. Given the impact of gamma oscillations on perception, motor function, memory, and emotion, external sensory stimuli can be employed to enhance or restore gamma activity, thereby improving cognitive function [7][8]. Existing theoretical frameworks support using sensory stimuli to evoke gamma oscillations, advancing this approach as a non-invasive, cost-effective, and clinically practical therapeutic strategy, accelerating its translation for diagnosing and treating disorders of consciousness.

2. System Design Requirements

The primary function of the 40 Hz audiovisual intervention device is to deliver steady-state 40 Hz auditory and visual stimuli to modulate neural activity in the human brain, thereby inducing 40 Hz gamma oscillations for improving cognitive outcomes in patients with chronic disorders of consciousness. To ensure stimulation efficacy and safety considering individual variability and experimental conditions, the system must satisfy the following design requirements:

Audiovisual Stimulation Synchronization: Visual and auditory stimuli generally interact to maximize amplitude at specific phase angles [9]. Martorell A J et al. proposed that auditory and visual stimuli require onset alignment for 40 Hz multisensory stimulation in mice [10]. Clouter A et al. demonstrated that in human audiovisual stimulation [11], a slight temporal delay after visual stimulus onset is necessary due to differential neural processing times between senses (auditory responses being several milliseconds faster than visual responses) [12]. Based on these findings, the auditory stimulus onset in this device is delayed by 2 ms relative to visual stimulus onset to achieve relative audiovisual synchronization.

Audiovisual Stimulation Intensity: This parameter describes the relationship between sound and light intensities, typically used to determine their relative strengths. Intensity definitions relate to perceptual psychophysics, where subject-dependent perception defines the minimal detectable sound/light intensity ratio or perceived intensity ratio. Perceptual definitions are straightforward and practical. The intensity of 40 Hz audiovisual stimuli is adjustable based on subject responses via volume and luminance controls.

Audiovisual Pulse Width: Refers to the duration of individual sound and light pulses. Selection criteria depend on desired stimulation effects. Generally, longer pulse widths increase intensity but may cause sensory adaptation and fatigue, necessitating careful selection. Pulse width is also influenced by intensity, frequency, and duration parameters. Considering these factors, the device employs a 12.5 ms pulse width with 50% duty cycle.

The technical design parameters derived from these requirements are:

1) Operation mode: Synchronized audiovisual stimulation (visual stimulus precedes by 2 ms)
2) Output pulse frequency: Steady-state 40 Hz

3) Output pulse width: 12.5 ms
4) PWM dimming: Asymmetric bidirectional pulse wave
5) Speaker specifications: 60-80 dB; 1-10 kHz auditory clicks/tones
6) Blue LED specifications: Centroid wavelength 472 nm; irradiance 0.03 mW/cm²
7) Safety compliance: Class II equipment with internal power source, Type BF applied part per IEC 60601-1 requirements.

3. Design of the Overall System Hardware Scheme

This study proposes a 40 Hz gamma oscillation-based audiovisual intervention device primarily designed for consciousness recovery and cognitive improvement in patients with chronic disorders of consciousness. Building upon preliminary experiments, a specialized wearable eye mask was developed through circuit design and parameter optimization. The eye mask incorporates a lithium battery coupled with DC-DC conversion and low-dropout regulator circuits to establish one-touch power management. The main control module employs an STM32L1 series microcontroller to coordinate peripheral circuits—including an LED driver, digital-to-analog converter, and audio amplifier circuit—for delivering 40 Hz audiovisual stimulation.

3.1 Hardware Modules

3.1.1 DAC Module for Digital Audio

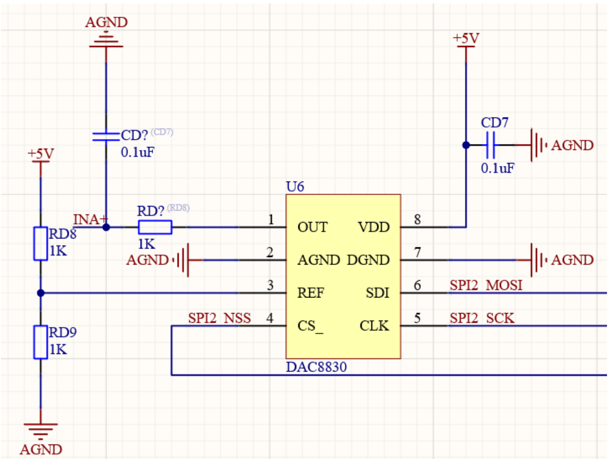

Figure 1: Schematic of the DAC Module

In digital audio systems, the digital-to-analog converter (DAC) module constitutes a critical component, as its performance directly determines audio fidelity parameters including signal reconstruction quality and signal-to-noise ratio. Consequently, selecting a high-precision DAC module is essential for digital audio device design. This study employs Texas Instruments' DAC8830, a 16-bit resolution converter chip characterized by low power consumption, high accuracy, and rapid conversion rates, widely implemented in instrumentation and communication applications [13][14]. The DAC8830 supports four interface modes: serial, parallel, SPI, and QSPI. To fulfill system requirements, the SPI interface was selected for microcontroller unit interconnection, enabling digital waveform data transfer from Flash memory to the DAC for conversion. Ensuring post-conversion signal integrity and mitigating digital noise interference necessitate isolating analog and digital power supplies. During PCB design, cross-talk between digital and analog circuits must be minimized through optimized routing: signal traces should be shortened to reduce propagation delays, while appropriate filtering circuits suppress noise and harmonics. Voltage reference stability represents another critical factor; here, a 2.5V reference is derived via a resistor divider from a 5V linear regulator output. The circuit schematic of the DAC module is presented in Figure 1.

3.1.2 Audio Power Amplifier Circuit

The design of power amplifier circuits is critical in audio applications, aiming to amplify low-level audio signals to sufficient levels for driving speakers or other loads [15][16]. This study employs a Class-D amplifier topology to amplify 40 Hz audio signals. The Class-D amplifier architecture typically comprises an input switching stage, power amplification stage, and output filter stage. Operating in pulse-width modulation (PWM) mode, it converts audio signals into high-frequency switching signals by comparing the audio input against a high-frequency triangular wave via a comparator. When the voltage at the inverting input exceeds that of the non-inverting input, the output transitions low; conversely, it transitions high when the non-inverting input voltage is higher. The MIX3022 was selected as the Class-D audio amplifier for its superior noise performance and low total harmonic distortion plus noise (THD+N ≤ 0.04%), enabling high-fidelity signal amplification. After filtering the analog output from the DAC, the signal is fed into the left and right channels of the MIX3022. The schematic diagram of the audio power amplifier circuit is illustrated in Figure 2.

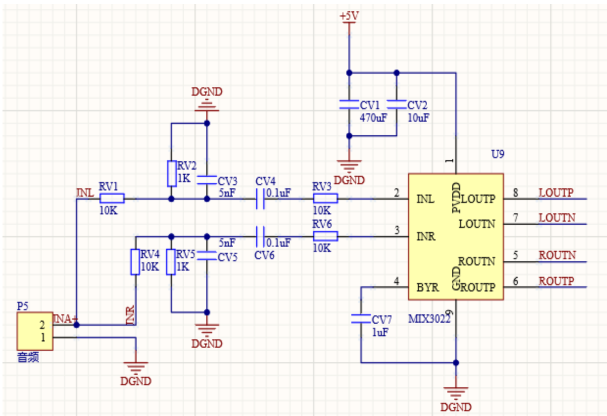

Figure 2: Schematic Diagram of the Audio Power Amplifier Module

3.1.2 LED Driver Circuit

The LED driver circuit module converts digital signals into stable output current through precise analog signal processing. Specifically, a digital-to-analog converter transforms digital input into analog voltage (Figure 3), which is fed to the non-inverting input of an operational amplifier configured as a feedback amplifier. This operational amplifier regulates the output current via a negative feedback loop incorporating a resistor and PN-junction transistor. When the DAC output voltage varies, the feedback mechanism adjusts the current source output accordingly. The current source circuit employs a voltage comparator and output stage. To achieve the 40 Hz flicker frequency required for LED stimulation, PWM dimming is implemented with a 4.99 Ω current-sense resistor. A 4V 40 Hz PWM waveform from the DAC establishes an

800 mA operating current, enabling stable operation of 3W LEDs (±0.8% current accuracy). Critical design considerations include selecting DAC resolution (>16-bit) and operational amplifier gain (≥100 dB) to ensure target current range precision, while accounting for component tolerances and thermal stability.

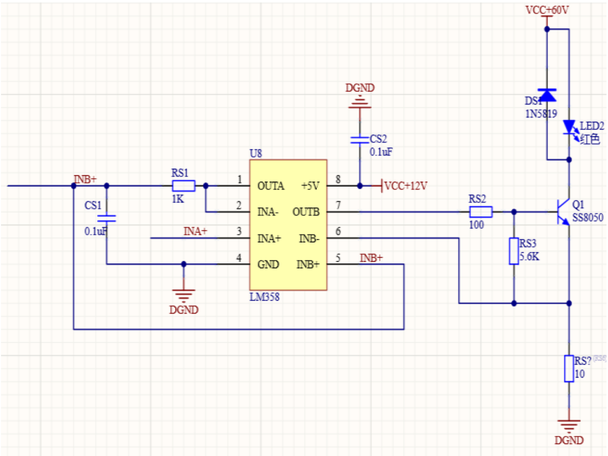

Figure 3: Schematic of the LED Driver Circuit

3.2 Software Modules

3.2.1 Generation of Brainwave Music

A lookup table method was implemented to store a 40 Hz amplitude-modulated audio signal with 1 kHz carrier frequency in the microcontroller's FLASH memory. Per the Nyquist-Shannon sampling theorem, the sampling rate must exceed twice the highest signal frequency component (1 kHz). Thus, a minimum 2 kHz sampling rate was required. To enhance output signal fidelity, a 4 kHz sampling rate was selected.

The digital signal was generated by computing signal amplitudes at each sampling point, storing these values as an array in FLASH. Each array element represents the signal amplitude at a specific timestamp, with array length determined by sampling rate and signal duration.

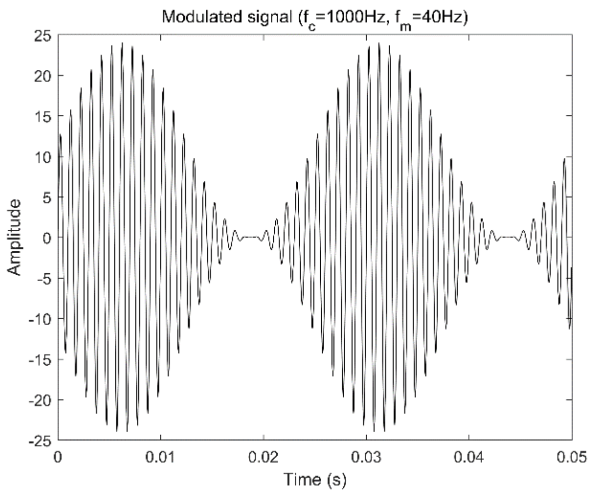

Figure 4: Waveform Diagram of Simulated Brainwave-Modulated Audio

Signal reconstruction employed the lookup table approach: A timer triggered interrupts at 4 kHz intervals (matching the sampling rate). During each interrupt service routine, the current amplitude value was retrieved from the FLASH array and output to the DAC. As shown in Figure 4, the generated waveform exhibited negligible distortion, confirming proper modulation implementation.

3.2.2 Design of Audiovisual Synchronization

Audiovisual synchronization is the focal point of gamma oscillation intervention devices. Its implementation mechanism relies on the difference in neural processing times for auditory and visual sensations in humans, specifically that auditory responses are several milliseconds faster than visual responses. Therefore, to achieve therapeutic effects, the design of audiovisual intervention devices must address the requirement for relative audiovisual synchronization. In this regard, research by Clouter A et al. indicates that delaying auditory stimulus onset by 2 ms relative to visual stimulus onset is a feasible solution [17][18].

Synchronization is achieved by linking the audio signal envelope to the light source switching. Specifically, a timer generates PWM signals with two primary parameters: switching frequency and duty cycle. The PWM switching frequency represents the flicker frequency of light stimulation, while the duty cycle represents the light pulse width within one light stimulation cycle.

Based on experimental requirements in this study, the PWM frequency is set to 40 Hz (period = 25 ms) by configuring the microcontroller’s TIMx_ARR and TIMx_CCR registers. In PWM up-counting mode, the output pin is driven LOW when the timer counter value is less than the compare value, and HIGH otherwise. Setting the compare value to half of the counter’s upper limit achieves a 50% duty cycle (light stimulation pulse width = 12.5 ms).

As the auditory stimulus envelope is modulated at 40 Hz, auditory stimulation starts 2 ms after light stimulation initiation. When the counter reaches the preset compare value, the program enters a timer interrupt. After 2 ms, the interrupt service routine reads the array stored in FLASH and outputs values to the DAC. This fulfills the requirement for relative audiovisual synchronization. The implementation principle is illustrated in Figure 5.

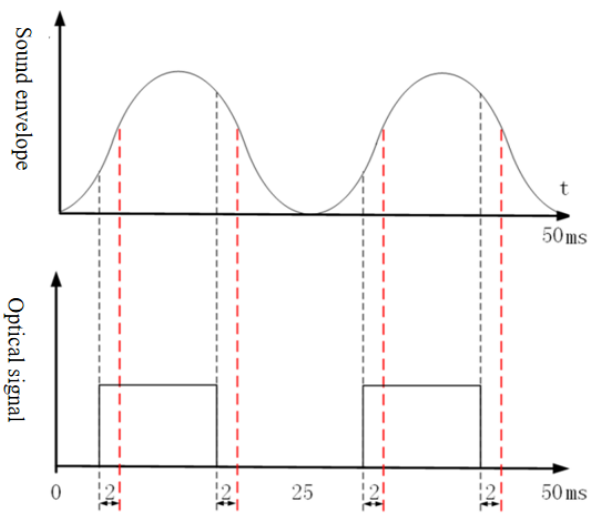

Figure 5: Schematic Diagram of the Audiovisual Synchronization Implementation

3.3 Structural Design and Physical Implementation of the Eye Mask

To meet experimental requirements, a wearable eye mask was designed, primarily fabricated from ABS stereolithography resin UTR9000. The contact surface incorporates soft sponge-stitched cotton fabric to ensure comfort. To prevent light leakage into the eyes, high-brightness, low-power-consumption LEDs with extended longevity are embedded within the mask housing. These LEDs are coupled with light-cured resin lenses polished for optical precision. For auditory stimulation, miniature speakers integrated into the mask employ bone conduction to transmit sound to the inner ear, eliminating the need for ear canal insertion and making them ideally suited for this application. The overall 3D structure and physical implementation of the eye mask are presented in Figure 6.

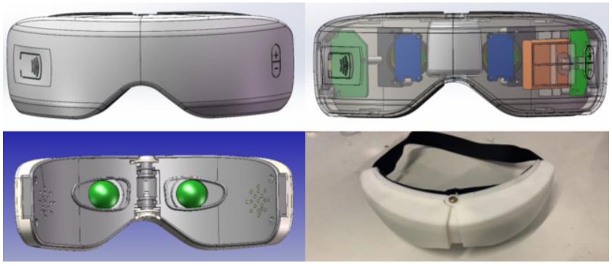

Figure 6: 3D Structural Diagram and Physical Implementation of the Eye Mask

4. Result

4.1 Characterization of Audio Stimulus Output Waveforms

The audio testing protocol evaluates the V/I conversion accuracy of the voltage-controlled constant-current source by measuring output waveform amplitude. With a 1 Ω current-sense resistor, an ammeter is connected in series with the load terminal. DC input voltages are applied, and the DAC output voltage readings are recorded alongside corresponding ammeter measurements. The experimentally obtained data with the 1 Ω sense resistor are listed in Table 1. The test results demonstrate excellent linearity and accuracy in voltage-to-current conversion, with measured output currents of 0-199.1 mA corresponding to input voltages of 0-200 mV, showing less than 1% error across the full range (maximum 0.98% at 50 mV input) and achieving best precision of 0.15% error at 200 mV input.

Table 1: Measured Data of the Voltage-Controlled Constant-Current Source

Setting the Voltage (mv)	0	50	100	150	200
Expected Current (mA)	0	50	100	150	200
Output Voltage (mV)	0	51.4	98.2	147.5	198.8
Actual Current (mA)	0	50.9	99.1	148.0	199.1
Error (%)	0	0.98	0.91	0.34	0.15

4.2 Characterization of 40 Hz Audio Output

The output of the audio power amplifier circuit was monitored using an oscilloscope, as illustrated in Figure 76. Under the 40 Hz analog audio output requirements, the analog signal exhibited satisfactory performance: waveform amplitude modulation and frequency (40 Hz ±0.5%) complied with preset parameters, while temporal precision confirmed auditory stimulus onset at 2 ms (±0.1 ms) after visual stimulus initiation. The signal largely preserved its morphological characteristics, though minor waveform irregularities were observed. These distortions are likely attributed to power supply instability from the battery source and DC offset voltage effects in the audio amplifier stage.

Figure 7: Audio Output Characterization Results

5. Conclude

This study developed and implemented a gamma oscillation-based audiovisual intervention device. By integrating peripheral circuits—including the audio power amplifier, LED driver, and PWM waveform output circuitry—a synchronized audiovisual stimulation system was successfully established. Hardware validation confirmed the device's capability for steady-state 40 Hz audiovisual stimulus output, with optical irradiance (0.03 mW/cm²) and auditory intensity (60-80 dB) complying with Class II Type BF medical safety standards per IEC 60601-1 requirements.

References

[1] Adrian E. Olfactory reactions in the brain of the hedgehog[J]. J Physiol, 1942, 100(4):459-473.

[2] Guan A, Wang S, Qiu C, et al. The role of gamma oscillations in central nervous system diseases: Mechanism and treatment[J]. Frontiers in Cellular Neuroscience, 2022, 10(2): 407.

[3] Rojas-Líbano, Daniel, and Leslie M. Kay. "Olfactory system gamma oscillations: the physiological dissection of a cognitive neural system." Cognitive Neurodynamics 2 (2008): 179-194.

[4] Strüber, Daniel, and Christoph S. Herrmann. "Gamma activity in sensory and cognitive processing." *The Oxford Handbook of EEG Frequency* (2022): 145-C8.

[5] Iaccarino H F, Singer A C, Martorell A J, et al. Gamma frequency entrainment attenuates amyloid load and modifies microglia[J]. Nature, 2016, 540(7632): 230-235.

[6] Schroeder C E, Lakatos P. The gamma oscillation: master or slave?[J]. Brain topography, 2009, 22: 24-26.

[7] Adaikkan C, Middleton S J, Marco A, et al. Gamma Entrainment Binds Higher-Order Brain Regions and Offers Neuroprotection[J]. Neuron, 2019, 102(5): 929-943.e8.

[8] Fernandez-Ruiz A, Sirota A, Lopes-dos-Santos V, et al. Over and above frequency: Gamma oscillations as units

of neural circuit operations[J]. Neuron, 2023, 111(7): 936-953.

[9] Lustenberger C, Patel Y A, Alagapan S, et al. High-density EEG characterization of brain responses to auditory rhythmic stimuli during wakefulness and NREM sleep[J]. Neuroimage, 2018, 169:57-68.

[10] Martorell A J, Paulson A L, Suk H J, et al. Multi-sensory Gamma Stimulation Ameliorates Alzheimer's - Associated Pathology and Improves Cognition[J]. Cell, 2019, 177(2): 256-271. e22.

[11] Pastor M A, Artieda J, Arbizu J, et al. Activation of human cerebral and cerebellar cortex by auditory stimulation at 40 Hz[J]. Journal of Neuroscience the Official Journal of the Society for Neuroscience, 2002, 22(23):10501.

[12] Clouter A, Shapiro K L, Hanslmayr S. Theta Phase Synchronization Is the Glue that Binds Human Associative Memory[J]. Current Biology, 2017, 27(20): 3143-3148. e6.

[13] Chuanxi, J, Liu Minghui, and Chen Panhui. "Design of a Multi-Channel Expandable High-Precision Isolated Current Source Module." *Journal of Physics: Conference Series*. Vol. 1971. No. 1. IOP Publishing, 2021.

[14] Wang, Feihu, Zhaohui Hu, and **n Liu. "Low Noise VCSEL Driver for SERF Atomic Magnetometer." IOP Conference Series: Materials Science and Engineering. Vol. 711. No. 1. IOP Publishing, 2020.

[15] Self, Douglas. *Audio power amplifier design*. Routledge, 2013.

[16] Mei, Shangming, et al. "The class D audio power amplifier: A review." *Electronics* 11.19 (2022): 3244.

[17] Romei, Vincenzo, et al. "Auditory stimulus timing influences perceived duration of co-occurring visual stimuli." *Frontiers in psychology* 2 (2011): 215.

[18] Clouter, Andrew, Kimron L. Shapiro, and Simon Hanslmayr. "Theta phase synchronization is the glue that binds human associative memory." Current Biology 27.20 (2017): 3143-3148.